



LAWRENCE
LIVERMORE
NATIONAL
LABORATORY

A minimum turbulence state for coarse grained simulation

Y. K. Zhou

January 23, 2015

11th. World Congress on Computational Mechanics
Barcelona, Spain
July 20, 2014 through July 25, 2014

Disclaimer

This document was prepared as an account of work sponsored by an agency of the United States government. Neither the United States government nor Lawrence Livermore National Security, LLC, nor any of their employees makes any warranty, expressed or implied, or assumes any legal liability or responsibility for the accuracy, completeness, or usefulness of any information, apparatus, product, or process disclosed, or represents that its use would not infringe privately owned rights. Reference herein to any specific commercial product, process, or service by trade name, trademark, manufacturer, or otherwise does not necessarily constitute or imply its endorsement, recommendation, or favoring by the United States government or Lawrence Livermore National Security, LLC. The views and opinions of authors expressed herein do not necessarily state or reflect those of the United States government or Lawrence Livermore National Security, LLC, and shall not be used for advertising or product endorsement purposes.

A minimum turbulence state for coarse grained simulation

Ye Zhou

Lawrence Livermore National Laboratory
Livermore, CA 94550, USA

1. INTRODUCTION AND SUMMARY

In many problems in fundamental physics, we must simultaneously deal with uncertainty in the underlying equations of motion and with uncertainty in our ability to solve them. In turbulence, we have only the latter [1]. As noted by renowned physicist Richard Feynman, the turbulence problem is still referred to as the last unresolved classical physics problem [2].

The presence of strong nonlinear interactions makes turbulence a truly multiple scale problem. The challenge in direct numerical simulations (DNS) of a very high Reynolds number flow is to account for all the scales, starting from the largest where the energy injection occurs to scales that are roughly two times the Kolmogorov dissipation wavenumber. The Reynolds number, Re , is around 10^8 for airplane wing and fuselage [3] and even higher for turbulent flows in space and astrophysical setting [4]. Specifically, the Reynolds number, which is the ratio between the inertial forces to the viscous actions, is defined as

$$Re = UL/\nu \quad -- \quad (1)$$

where U , L are the characteristic velocity and length scales, and ν is the kinetic viscosity [5].

Fig. 1 shows the distinctive spectral scales from a large collection of the wind tunnel and geophysical experiments (reproduced from Ref. 6).

In such a computationally intensive field, we have witnessed an unprecedented advancement of the capabilities of the supercomputers. For grid generated turbulence or turbulent flows in a periodic box, brute-force DNS has already matched or surpassed experiments [7]. Pope [8] even suggested that we have entered an era of sufficient computer power.

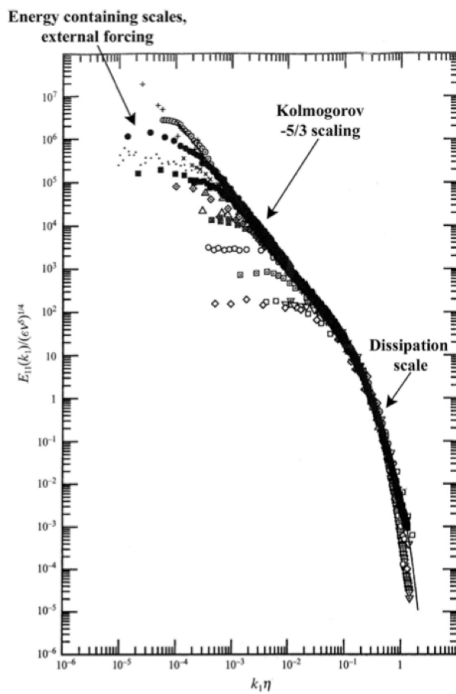


Fig. 1. The compensated longitudinal energy spectra are plotted against the longitudinal wavenumbers. The data are obtained from a collection of the wind tunnel and geophysical flows (reproduced from Ref. 6, with permission from Cambridge Univ. Press). The values of the Reynolds numbers are based on the Taylor microscales.

In this chapter, the classical “turbulence problem” is narrowed down and redefined for scientific and engineering applications. From an application perspective, accurate computation of large-scale transport of the turbulent flows is needed. Here, an analysis that allows for the large-scales of very high Reynolds number turbulent flows to be handled by the available supercomputers is inspected. Current understanding of the energy transfer process of the turbulent flows, which forms the foundation of our argument, is discussed. Two distinctive interactions, namely, the distance and near-grid interactions, are inspected for large-scale simulations. The distant interactions in the subgrid scales in an inertial range can be effectively modelled by an eddy damping. The near-grid interactions must be carefully incorporated. The data redundancy in the inertial range is demonstrated.

Furthermore, the minimum state is defined as the turbulent flow which has the lowest Reynolds number that captures the energy containing scales of the astrophysics problems in a laboratory or simulation setting. The transition criterion for the time-dependent flows is presented.

Two types of applications are briefly summarized. First of all, the spatial and temporal criterions have found applications to a range of high energy density physics experiments. Secondly, the procedure for estimating the numerical viscosity for implicit large-eddy simulations (ILES) has been advanced.

2. “TURBULENCE PROBLEM” REDEFINED

Most important properties of a high Reynolds number turbulent flow are determined by the transport dynamics of the large-scales. Therefore, it makes sense to focus computing resources on capturing these scales accurately. From an application perspective, accurate and time-dependent, three-dimensional computations of the large-scales may be all that is needed. It is therefore necessary to choose the grid-size in a uniform fashion, using the boundary between the large-scales and inertial range.

In support of this argument, it will be illustrated that the self-similarity properties lead to the data redundancy; an advantage that should be fully exploited. The universality of the inertial range is indeed remarkable. At high Reynolds number, this universality can be observed by the establishment of an extended inertial range (Fig. 1) or the asymptotic behaviour of the normalized energy dissipation rate. Indeed, the characteristic time scale of the energy containing eddies, U/L , should be in the same order of magnitude as the time scale of the energy dissipation rate ε/U^2 . Here, the energy dissipation rate is denoted as ε . Therefore, a dimensionless ratio, D , can be introduced as,

$$D = \varepsilon L / U^3. \quad (2)$$

Recently, a significantly amount work has been devoted to investigate the behaviour of D as a function of Re [see Figs. 2 and 3; Refs. 9-13].

This article notes that (1) two distinct interactions have been identified; (2) a model that incorporates both interactions already exists; (3) a refined boundary between the energy containing and inertial ranges can be located; (4) the self-similarity in the inertial range has been demonstrated. As a result, a scaling argument to scale the extremely high Reynolds number flows to high, but manageable Reynolds number in order to fit into the existing supercomputers is proposed.

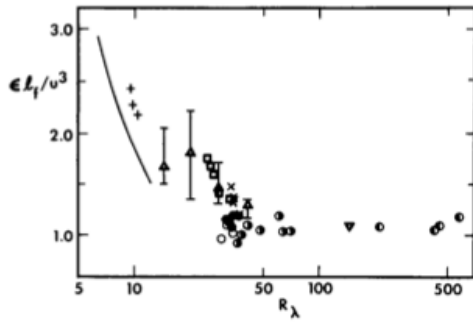


Fig. 2. Non-dimensional parameters: (a) $\varepsilon l_f/u^3$ based on laboratory data, with l_f denoting a longitudinal integral scale – from Ref. [11], with L denoting the integral scale.

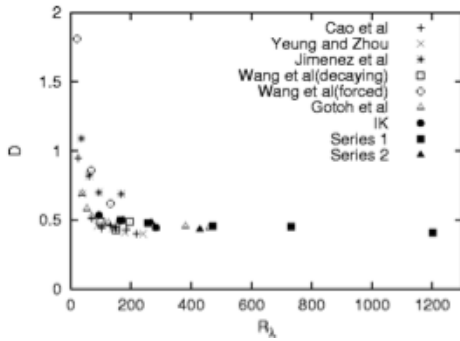


Fig. 3. Non-dimensional parameters: $D = \varepsilon L/u^3$ based on computational simulation data – from Ref. [12], with L denoting the integral scale.

A. Filter classification and their spectral support

The objective of the filters is to separate the large-scales as faithfully as possible. Therefore, the filtering operation, which divides the flow into the subgrid and resolvable scales, should not adversely affect the large-scale properties.

Zhou *et al.* [14] pointed out that the resolvable scale interactions are affected when the filters with same spectral support are utilized. The so called “Type A category” filters include familiar

Gaussian [15] and exponential filters [16]. The subgrid scale field, as well as the subgrid stresses, can be directly evaluated from the resolvable scale field (see for example, References 17-19).

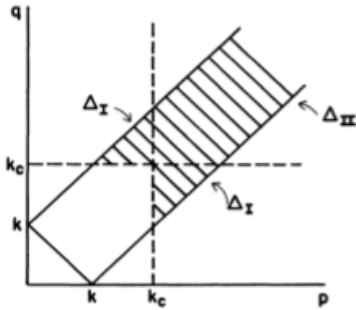


Fig. 4. Region of integration for the sharp-cut filter (from Ref. 20)

However, in LES implementation, the maximum wavenumber is determined by the grid size. For wavenumber up the cutoff, k_c , all functions, the original, resolvable, and subgrid, are known. Nothing is known for $k > k_c$. The sharp cutoff filter (the “Type B category”) has distinctive spectral support (Ref. 14).

B. Near-grid and distant interactions

As noted already, from an application perspective, the time-dependent, three-dimensional computations of the energy-containing scales may be all that is needed. Using a sharp cutoff filter, the subgrid of a given problem can be subdivided into two distinctive areas. The resolvable scale wavenumber is denoted k which satisfies a triad $\mathbf{k}=\mathbf{p}+\mathbf{q}$. The subgrid region for *the near-grid interactions*, where one of the wavenumber is greater and the other is less than the cutoff wavenumber, k_c , is denoted as Δ_I . The subgrid region where both wavenumbers are greater than k_c (*the distant interaction region*), is denoted as Δ_{II} . Detailed studies of subgrid models in the energy transfer and momentum equations reveal the relationship between the eddy damping, backscatter and the Reynolds and cross stresses [20].

The near-grid and distant interactions plays distinctive roles in the energy transfer process [21]. The eddy viscosity $\nu^{>>}(k)$, resulting from the distant interactions, behaves in the same manner as the molecular viscosity. Therefore, an eddy viscosity model is acceptable. The eddy viscosity $\nu^{<<}(k)$,

resulting from the near-grid interactions, is responsible for the cusp-like behaviour of the spectral eddy viscosity first identified by Kraichnan [22] (Fig. 5).

To confirm the importance of the near-grid interaction dynamics, the model equation should be accurately resolved [23]. In an illustrative example, a fictitious cutoff wavenumber is introduced in a DNS and the near-grid interactions between the resolvable and subgrid scales are kept. Again, the results demonstrated that the near-grid interactions are critical for faithful computation of the large-scale evolutions.

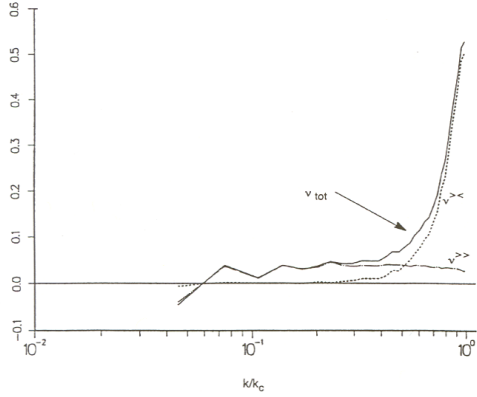


Fig. 5. Spectral eddy viscosity and the individual contributions from both the near-grid and distant interactions (from ref. 21)

C. Resolvable scale model equation

The first order of business is to derive a resolvable scale equation using the method of recursive renormalization (r-RG) group theory. This methodology was first proposed by Rose [24] for a model problem of passive scalar advection and was extended to Navier-Stokes equation [25-26]. Starting from the Kolmogorov dissipation wavenumber, the inertial range is divided into multiple shells, with their length as thin as possible. The first resolvable scale equation can be written symbolically as (P denotes the projection operator)

$$\partial u^</\partial t + \nu_0 k^2 u^< = P [u^< u^< + 2 u^< u^> + u^> u^>] . \quad -- (3)$$

After removing the first subgrid shell, two types of subgrid interactions will make their distinctive contributions, and hence, they must be considered individually. First, the distant interactions (the

last term on the right hand of Eq. 3) will result in an enhanced eddy viscosity, ν_1 . Second, the near-grid interaction (the second term on the right hand of Eq. 3) should be either computed directly, or approximated by an expression in the resolvable scale field. This process is repeated to remove the remaining subgrid scales shells.

The resulting recursion relation for these subgrid-subgrid scale interactions lead to a fixed point--the eddy viscosity. For a large-eddy simulation (LES) model, the near-grid interactions should be considered explicitly

$$\partial \overline{u^2} / \partial t + \nu_{eff} k^2 \overline{u^2} = P [\overline{u^2} + 2 \overline{u^2} \overline{u^2}]. \quad \text{--- (4)}$$

The wavenumber domain for the left hand side of (4) and the first term on the right hand side is $[0, k^*]$, while that for the second term is $[0, 2k^*]$. Here, k^* is used to denote the boundary between the energy containing and inertial ranges, which will be defined more precisely in the next section. The eddy viscosity, ν_{eff} , should have contributions from both the subgrid-subgrid and subgrid-resolvable scale interactions.

3. COARSE GRAINED SIMULATIONS

A. Determination of the boundary between the energy containing and inertial ranges

The traditional definition of the inertial range is the existence of a scale which is free from the large-scale forcing and small-scale viscous dissipation. A more precise definition can be introduced, where the upper and lower boundaries of the inertial range depend on the outer-scale (δ) and Reynolds number [27-30]:

$$\text{Lower bound:} \quad L \nu \approx 50 \text{ Re}^{-3/4} \delta, \quad \text{--- (5)}$$

$$\text{Upper bound:} \quad L_{L-T} \approx 5 \text{ Re}^{-1/2} \delta. \quad \text{--- (6)}$$

It is well known that $\text{Re} > 10^4$ (Hinze, [31]), (or 100 when the Taylor microscale is used) is needed for an inertial range.

The upper bound of the inertial range in this LES model for resolvable scale equation is our minimum grid size, which can be chosen as the grid-size in physical space or cutoff wavenumber in spectral space.

B. Data redundant in the inertial range

How can we compute the large-scale of these higher Reynolds numbers turbulent flows found in astrophysical or geophysical flows? The answer lies in the universality of the inertial range, which we should exploit and utilize.

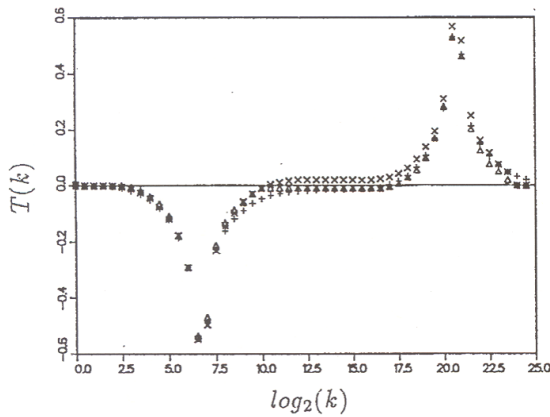


Fig. 6. The energy transfer function of different grid sides for idealized Kolmogorov inertial range wavenumber. Rescaled to illustrate the “pipe without leak” analogy (from References 33-34)

In fact, the universality in the inertial range can be demonstrated by computing the triadic energy transfer functions (for definition, see, for example, Domaradzki and Rogallo [32]). In Zhou [33-35], these triadic interactions are selected such that they satisfy the self-similarity scaling laws of Kraichnan [36]. The reconstructed energy transfer function, $T(k)$, based on calculations for several grid sizes, has been shown to differ only in its range (or extent) in the spectral domain. With a given energy input, this ideal Kolmogorov inertial range is essentially a pipe without leak. The different length of the pipe only reflects the different resolutions (or in other words, different Reynolds number) of the flows (Fig. 6).

Based on this understanding, one can rescale these energy transfer function without affecting the large-scale. This is the clear evidence of data redundancy in the inertial range.

C. Local and non-local interactions in high Reynolds number flows

What would be the minimum resolution requirement (minimum model) for a faithful model calculation of the large-scale of a flow? The answer is that the near-grid interactions must be in the inertial range. The condition for this requirement can be found by demanding that the upper wavenumber of the near-grid scale, $2k_c$, be equal to the lower boundary of the inertial range_v (inner viscous scale).

In order to separate the local and nonlocal interactions, the so-called ‘disparity’ parameter [33-35]

$$s(k,p,q) = \max(k,p,q)/\min(k,p,q) \quad -(7)$$

is employed. In spectral space, the wavenumber \mathbf{k} satisfies a triad $\mathbf{k}=\mathbf{p}+\mathbf{q}$. This parameter has been used to classify the interactions as local ($s \sim 2$) and nonlocal ($s > 2$) by Lesieur [37].

In the inertial range, the fractional energy flux for a given wavenumber scales vs the scale disparity parameter has been determined to follow a -4/3 power law (References 33-35; see Fig. 7)

$$\Pi(k,s)/\Pi(k) \sim s^{-4/3} \quad -(8)$$

The work by Gotoh and Watanabe [38] also provided support to this scaling law. These authors used both direct numerical simulations and a statistical closure theory, the Lagrangian Renormalized Approximation (LRA) (Kaneda [39]).

The peak of a normalized flux function can be found along with the value of s at which it occurs, s_p . Let’s also denotes s_h as the scale disparity parameter where the normalized flux reduces to half of its peak value [28, 40-41], i.e., $\Pi(k, s_h) = (1/2) \Pi(k, s_p)$. The scaling law can be rewritten as

$$s_h / s_p = 2^{(1/M)} \quad -(9)$$

As a result, the range of interactions one must keep is $[k_{L-T}, 2 k_{L-T}]$ as a result of $S_h / S_p = 2$.

Finally, several published numerical works by Domaradzki *et al.* [42-43] also suggested the specific length of the inertial range that one must keep. These authors have numerically investigated isotropic and anisotropic channel flows. They found that the modes that are smaller than a fictitious cutoff wave number k_C will not extend their interactions beyond $2k_C$.

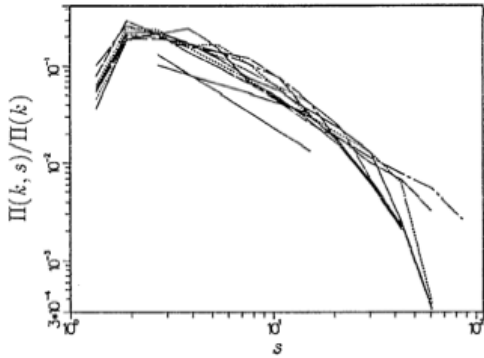


Fig. 7. Fractional contribution $\Pi(k,s)/\Pi(k)$ from simulated datasets. The various curves are for $k=2^{n-2}$, $6 < n < 14$. The straight lines indicate $s^{-2/3}$ and se^{-4} behaviors [References 33-34].

4. THE MINIMUM STATE

The mixing transition concept for *stationary* fluid flows refers to the transition to a turbulent state in which the flow drives rapid mixing at the molecular scale. This turbulent state leads to rapid dissipation of momentum and of concentration fluctuations (mixing). The extent of the effective inertial range could be narrowed to [27,28]

$$\lambda_K < \lambda_v \ll \lambda \ll \lambda_{L-T} < \delta, \quad --(10)$$

Here the lower-limit of the inertial range is the inner viscous scale $\lambda_v = 50\lambda_K$, where the Kolmogorov microscale can be rewritten as $\lambda_K = \delta Re^{-3/4}$. The upper-limit of the inertial range is the Liepmann-Taylor scale $\lambda_{L-T} = 5\lambda_T$, where $\lambda_T = \delta Re^{-1/2}$ is the well known Taylor correlation microscale [5].

To ensure the integrity of the physics of the large-scale dynamics of the flows of practical interest, the corresponding large-scale modes computed or measured in a simulation or a laboratory setting should not be contaminated because of their interaction with the dissipation range, which is not universal (Martinez et al., [44]). This requirement can be satisfied by maintaining a sufficiently broad inertial range. The required length of the inertial range needed can be deduced, for example, from our understanding of the interacting scales discussed in the previous section.

The *minimum state* is defined as the turbulent flow which has the *lowest* Reynolds number that captures the energy containing scales of the astrophysics problems in a laboratory or simulation setting (Zhou, [28,40-41]). The *minimum state* is therefore the lowest Reynolds number turbulent flow where all the modes in the energy containing scales will only interact with modes in the same spectral range or those within the inertial range. Obviously, this requirement is introduced to take full advantage of the universality of the inertial range.

The *minimum state*, according to the foregoing analysis, is the turbulent flow that takes the value of $k^*_Z \equiv 2 k^*_{L-T}$ equal to the inner-viscous wavenumber, k_{v_v} (the end of the inertial range, see Fig. 8). Using the definition of k_{L-T} and k_v , one finds that the *critical* Reynolds number of the *minimum state* is

$$Re^* = 1.6 \times 10^5. \quad --(11)$$

The outer-scale Reynolds number is approximately related to the Taylor microscale Reynolds number by $R_\lambda = (20/3)^{1/2} Re^{1/2}$ in isotropic flow. As a result, the corresponding *critical* Taylor-microscale Reynolds number of the *minimum state* is $R_\lambda^* \approx 1.4 \times Re^{1/2}$ ($R_\lambda^* \approx 560$).

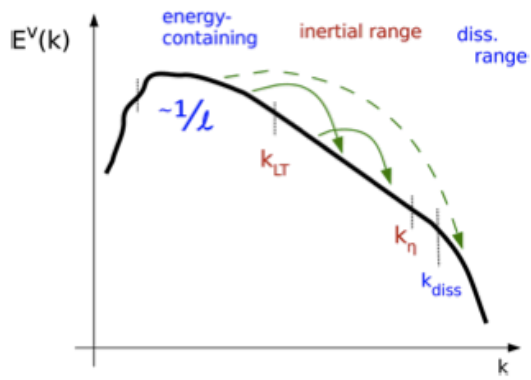


Fig. 8. (Color online) Sketch of a kinetic energy spectrum indicating the energy-containing, inertial, and dissipation ranges and their wavenumber boundaries. The idea behind the minimum state is that the inertial range should be long enough so that direct interactions between modes in the energy-containing and dissipation ranges are energetically weak, indicated by the dashed (green) arrow. Some “strong” interactions are indicated via the solid (green) arrows (Reference [40]).

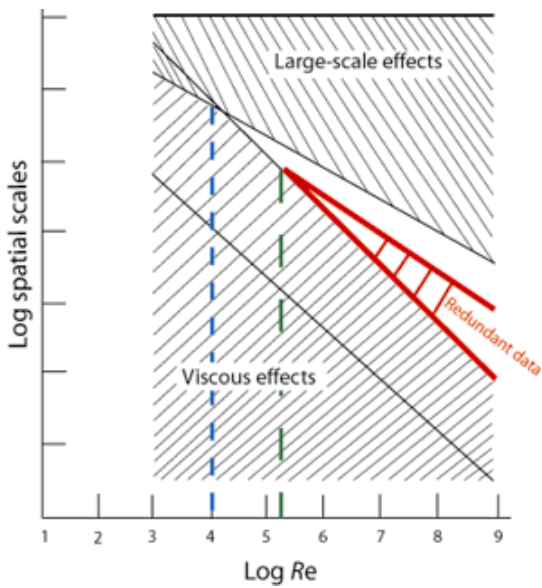


Fig. 9. An illustration of how an arbitrarily high Reynolds number flows can be scaled down to a manageable one (shown in green), but still captures the physics of the large-scale. Based on a figure in Dimotakis [27] with added marks in colour (Ref. [28]).

Fig. 9 provides another way to illustrate this argument using the physical length scales variation with the Reynolds number. The Reynolds numbers where an inertial range first occurs and the “*minimum state*” [28] are marked blue and green, respectively. The shaded area represents the redundant data of the inertial range. As a result, any high Reynolds number flow can be easily scaled down to a very high, but computationally achievable Reynolds number flow.

B. Temporal criterion

Many experiments have been conducted in classical fluid dynamics facilities, shock tubes, and laser facilities (such as the Omega laser and National Ignition Facility) to understand the complex flows induced by various instabilities. For example, the published examples were specialized to the Rayleigh-Taylor [45-46], Richtmyer-Meshkov [47-48] and Kelvin–Helmholtz flows [49]. Due to diagnostic limitations typical measurements consist solely of the growth of the mixing zone width. While these widths (of the bubble and spike fronts, individually or combined) are usually measured, it is difficult to know whether or not a particular experiment has reached mixing transition.

We have extended the stationary mixing transition to time-dependent flows and applied it to a wide range of experiments [29,30]. The Liepmann-Taylor scale essentially describes the internal laminar vorticity growth layer generated by viscous shear along the boundaries of a large-scale feature of size δ . The temporal development of such a laminar viscous layer is well known to go as $(\nu t)^{1/2}$ (Stokes [50], Lamb [51]).

$$\lambda_D = C (\nu t)^{1/2} \quad --(12)$$

Hence, the upper bound of the developing inertial range is the smaller of the Liepmann-Taylor scale, λ_{L-T} and λ_D . Here the coefficient of the diffusion layer, C , was suggested as $C \approx \sqrt{15}$ both for isotropic, homogeneous turbulence [52] and for steady parallel flows, and as $C \equiv 5$ for laminar boundary layer flows (Dimotakis [27]).

The inertial range is presumed to be established when the evolution of the large-scale, $\min\{\lambda_D, \lambda_{L-T}\}$, is decoupled from the inner viscous scale, λ_ν . For time-dependent flows, the mixing transition is achieved when a range of scales exists such that the temporally evolving

upper bound $[\min\{\lambda_D, \lambda_{L-T}\}]$ is significantly larger than the temporally evolving lower bound, λ_v . Thus, the mixing transition occurs if and when the inequality

$$\min\{\lambda_{L-T}(t), \lambda_D(t)\} > \lambda_v(t) \equiv 50\lambda_k(t)$$

--(13)

is satisfied (References 28, 40,41).

In designing and interpreting experiments for time-dependent flows, the time-dependent mixing transition provided the desirable ability to estimate the time required to achieve the mixing transition state.

5. APPLICATIONS

A. High energy density physics experiments

Achieving the minimum state should be a desirable goal for high energy density physics (HEDP) experimentalist when designing and developing their investigations. The Reynolds number of the minimum state may be achievable already for some of the most advanced experimental platforms [53-64].

The theoretical analysis for a HEDP experiment to achieve the Reynolds number at the *minimum state* or beyond can be summarized. The viscosity is evaluated, the outer scale or the characteristic velocity is computed, and the Reynolds number is determined. For a time-dependent flows, several length scales should be evaluated in order to inspect whether the both Eqs. (11) and (13) are satisfied [28-30].

B. Implicit large-eddy simulations effective Reynolds number

The utility of implicit large-eddy simulations (ILES) for practical scientific and engineering simulations is clear. The more broadly defined ILES [65] generally uses high-resolution non-

oscillatory FV (NFV) algorithms to solve the unfiltered Euler or Navier-Stokes equations. Recently, an unique issue has been advanced for ILES: how one can estimate the values of the relevant effective viscosity (ν_{eff}) produced by the numerical method [66]. It is critical to make progress on this matter, and further formalizing the perceived abilities of ILES in computing high Re flow, would indeed offer significant values.

Since ILES is applied to a broad range of engineering and scientific applications, a scheme should be developed in the physical space. In this fashion, ν_{eff} can be written as

$$\nu_{eff} = \varepsilon / \Omega, \quad --(13)$$

where Ω is the enstrophy $\Omega = \omega^2 / 2$, and the vorticity $\boldsymbol{\omega} = \nabla \times \mathbf{u}$, can be readily evaluated based on the simulated velocity \mathbf{u} data. As noted in Ref. (66), the key to accurately estimating ν_{eff} is to find a way to do so away from the smallest scales of the simulated flow, where the numerically controlled dissipation takes place. Once the dissipation rate is obtained, ν_{eff} can be written down based on a dimensional argument.

The turbulent flows of practical interest are usually both high Re and complex. Yet, as a first cut, an interesting scheme can be developed from the following procedure:

- For a highly resolved ILES flow, the compensated inertial range occurs at lower spectral ranges. The bottleneck occurs as a plateau at higher wave numbers [67-71].
- The flux is still the only link between the energetic and dissipative scales of motion.
- The effective dissipations of the computations can be obtained directly from the inflow profiles of the inertial range energy transfer.

Hence, a methodology should be utilized to estimate the “input” of the energy into the energy transfer from the large-scales. The key is to carry out this estimation around the energy containing scales so that the small scale information, where the dissipation is controlled by the numerical methods, are not needed. Fortunately, a large body of experimentally and numerically generated data suggested that a non-dimensional parameter such as D approaches a constant when Re becomes sufficiently large (e.g., Figs. 2 and 3). We note that the outer-scale (L) based Re is approximately related to the Taylor microscale Re_λ , by $Re_\lambda \approx (20/3)^{1/2} \sqrt{Re_L}$ in isotropic flow, and by $Re_\lambda \approx 1.4 \sqrt{Re_L}$ for turbulence in the far field of a jet. The literature shows internal consistency between the establishment of an inertial range and the asymptotic behavior of $D \rightarrow D_\infty = \text{constant}$. The

laboratory data compiled by Sreenivasan [10,11] exhibited constancy for $Re_\lambda > 100$.

The collection of the computational data by Kaneda [12] and Sreenivasan [10,11] indicated that somewhat higher Re_λ is needed, perhaps around 200, for which the inertial range is about one decade; observed data scatter for lower Re (e.g., in Figs. 2 and 3) has been attributed to differences among forcing schemes, forced long-wavelength ranges, and box sizes. At high Re limit, the energy flux can be estimated directly

$$(15)$$

Recent high resolution ILES [72-75], show a limited inertial range of the kinetic energy spectrum as well as distinct flow features associated with high Re flows. The viscosity-independent dissipation rate may have been thus captured for these high resolution ILES flows, and a dimensional estimation such as $v_{eff} = \varepsilon / \Omega$ – through Eqs. (14) and (15) – may provide a reasonable v_{eff} in this context.

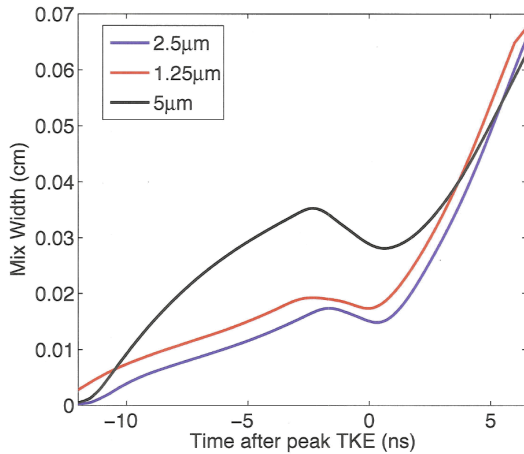


Figure 10. Asymptotic measures of the mixing width.

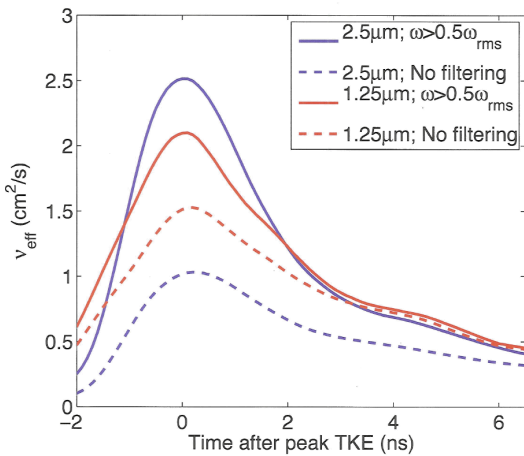


Fig. 11. Estimated effective eddy viscosity ν_{eff} .

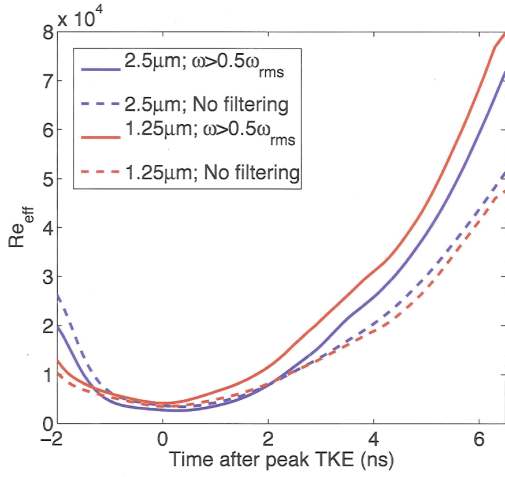


Fig. 12. Estimated outer-scale Re_{eff} .

The laboratory reshock experiments [55] were performed using the University of Rochester’s OMEGA laser. The laboratory target consists of a cylindrical beryllium (*Be*) tube ≈ 1.4 mm in length and ≈ 0.5 mm in diameter with a $\approx 100\mu\text{m}$ wall thickness. The target is successively hit from both sides by two laser-driven shocks. The first, ≈ 5 kJ, at $t = 0$ ns impacts the plastic ablator on the left, driving a Mach ≈ 5 shock through the $20\mu\text{m}$ aluminum (*Al*) tracer disk adjoining the ablator. The tracer disk is thus propelled to the right down the center of the cylinder, which is filled with a low-density (60mg/cc) *CH* foam. The second shock, ≈ 4 kJ at 5 ns, impacts a plastic ablator at the right end of the tube. The shocks collide at approximately 8 ns to the right of the mixing layer and reshock the mixing layer at approximately 10 ns, causing it to compress until approximately 13 ns. At approximately 17 ns, the second shock exits the mixing layer.

Asymptotic estimates for an outer-scale Re_{eff} can be also generated. Following the discussion, we assume that high Re isotropic turbulence regimes for which $D = \varepsilon L / U^3 \approx 1/2$ have been achieved,¹

¹ Following Kaneda et al. [12] (Fig. 3), we expect $D \sim 0.5 - 2$, with $D_\infty \approx 0.5$.

and define a time-dependent L to be the outer scale prescribed by a mixing width δ_{MZ} (Fig. 10). This mixing measure is designed to yield $\delta_{MZ} = h$ for $\psi(y) = 1 + \tanh(2(y - y_c)/h)$, where y_c defines the center of the mixing layer. We thus formulate an *asymptotic* model for the dissipation,

$\varepsilon = DU^3 / (2L)$; in this context we can now evaluate outer-scale (asymptotic) measures of

$v_{eff} = \varepsilon / [2 \langle s_{ij} s_{ij} \rangle]$ (Fig. 11), and $Re_{eff} = UL / v_{eff}$ (Fig. 12).

ACKNOWLEDGMENTS

This work was performed under the auspices of the Lawrence Livermore National Security, LLC under Contract No. DE-AC52-07NA27344.

BIBLIOGRAPHY

- [1] Nelkin, M., “*Universality and scaling in fully developed turbulence*,” Adv. in Phys., Vol. 43, pp. 143-181, 1994.
- [2] Zhou, Y., and Speziale, C.G., “*Advances in the fundamental aspects of turbulence, Energy transfer, interacting scales, and self-preservation in isotropic decay*,” Appl. Mech. Rev., Vol. 51, p. 267, 1998.
- [3] Moin, P., and Kim, J., “*Tracking turbulence with supercomputers*,” Scientific American, Vol. 276, pp. 62-68, 1997.
- [4] Zhou, Y., Matthaeus, W.H., and Dmitruk, P., “*Magnetohydrodynamic turbulence and time scales in astrophysical and space plasma*,” Rev. Mod. Phys., Vol. 76, pp. 1015-1035, 2004.
- [5] Batchelor, G.K., Theory of homogeneous turbulence, Cambridge University Press (Cambridge, UK, 1953)
- [6] Saddoughi, S.G., Veeravalli, S.V., *Local isotropy in turbulent boundary layers at high Reynolds number*. J. Fluid Mech. **268**, 333, 1994,
- [7] Jiménez, J., “*Computing high-Reynolds-number turbulence: will simulation ever replace experiments?*” J. Turbulence, Vol. 4, 022, pp.1-14, 2003.
- [8] Pope, S.B., “*Ten questions concerning the large-eddy simulation of turbulent flows*,” New J. Phys., Vol. 6, 35, pp. 1-24, 2004.
- [9] Burattini, P., Lavole, P., and Antonia, R.A., “*On the normalized energy dissipation rate*,” Phys. Fluids, Vol. 17, 098103, pp.1-4, 2005.
- [10] Sreenivasan, K.R., “*On the scaling of the turbulence energy dissipation rate*,” Phys. Fluids, Vol. 27, pp. 1048-1051, 1984
- [11] Sreenivasan, K.R., “*An update on the energy dissipation rate in isotropic turbulence*,” Phys. Fluids, Vol. 10, pp. 528-529, 1998.
- [12] Keneda, Y., Ishihara, T., Yokokawa, M., Itakura, K., and Uno, A., “*Energy dissipation rate and energy spectrum in high resolution direct numerical simulations of turbulence in a periodic box*,” Phys. Fluids, Vol. 15, L21-24, 2003.
- [13] Pearson, B.R., Krogstad, P.-A., and van de Water, W., “*Measurements of the turbulent energy dissipation rate*,” Phys. Fluids, Vol. 14, pp. 1288-1290, 2002.

- [14] Zhou, Y., Hossain, M., and Vahala, G., “*A critical look at the use of filters in large eddy simulation,*” Phys. Lett. A, Vol. 139, pp. 330-332, 1989.
- [15] Leonard, A., “*Energy cascade in large-eddy simulations of turbulent fluid flows,*” Adv. Geophy. S., 18A, pp. 237–248, 1974.
- [16] Germano, M., “*Differential filters for the large eddy simulation of turbulent flows,* Phys. Fluids, Vol. 29, pp. 1755-1757, 1986.
- [17] Langford, J.A., and Moser, R.D., “*Optimal LES formulations for isotropic turbulence,*” J. Fluid Mech., Vol. 398, pp. 321-346, 1999.
- [18] Domaradzki, J.A., and Loh, K.-C., “*The subgrid-scale estimation model in the physical space representation,*” Phys. Fluids, Vol. 11, pp. 2330-2342, 1999.
- [19] Domaradzki, J.A., and Adams, N.A., “*Direct modelling of subgrid scales of turbulence in large eddy simulations,*” J. of Turbulence, Vol. 3, 024, pp. 1-19, 2002.
- [20] Zhou, Y., “*Eddy damping, backscatter, and subgrid stresses in subgrid modeling of turbulence,*” Phys. Rev. A, Vol. 43, pp 7049-7052, 1991.
- [21] Zhou, Y., and Vahala, G., “*Reformulation of recursive-renormalization-group based subgrid modeling of turbulence,*” Phys. Rev. E, Vol. 47, pp. 2503-2519, 1993.
- [22] Kraichnan, R.H., “*Eddy viscosity in two and three dimensions,*” J. Atmos. Sci., Vol. 33, pp. 1521-1536, 1976.
- [23] Dubois, T., Jauberteau, F., and Zhou, Y., “*Influences of subgrid scale dynamics on resolvable scale statistics in large-eddy simulations,*” Physica D, Vol. 100, pp. 390-406, 1997.
- [24] Rose, H.A., “*Eddy diffusivity, eddy noise, and subgrid-scale modelling,*” J. Fluid Mech., Vol. 81, pp. 719-734, 1977.
- [25] Zhou, Y., Vahala, G., and Hossain, M., “*Renormalization-group theory for the eddy viscosity in subgrid modeling,*” Phys. Rev. A, Vol. 37, pp. 2590-2598, 1988.
- [26] Zhou, Y., Vahala, G., and Hossain, M., “*Renormalization eddy viscosity and Kolmogorov’s constant in forced Navier-Stokes turbulence,*” Phys. Rev. A., Vol. 40, pp. 5865-5874, 1989.
- [27] Dimotakis, P.E., “*The mixing transition in turbulent flows*”, J. Fluid Mech., Vol. 409, pp. 69-98, 2000.
- [28] Zhou, Y., “*Unification and extension of the concepts of similarity criteria and mixing transition for studying astrophysics using high energy density laboratory experiments or numerical simulations,*” Phys. Plasmas, **14**, 082701. 2007.
- [29] Zhou, Y., Robey, H.F., and Buckingham, A.C., “*Onset of turbulence in accelerated high-Reynolds-number flow,*” Phys. Rev. E, Vol. 67, 056305, pp. 1-11, 2003a.

- [30] Zhou, Y., Remington, B.A., Robey, H.F., *et al.*, “*Progress in understanding turbulent mixing induced by Rayleigh-Taylor and Richtmyer-Meshkov instability,*” *Phys. Plasma*, Vol. 10, pp. 1883-1896, 2003b.
- [31] Hinze, J.O., *Turbulence*, 2nd Edn, (McGraw-Hill, New York, 1975).
- [32] Domaradzki, J.A., and Rogallo, R.S., “*Local energy transfer and non-local interactions in homogeneous, isotropic turbulence,*” *Phys. Fluids A*, Vol. 2, pp.413-426, 1990.
- [33] Zhou, Y., “*Degree of locality of energy transfer in the inertial range,*” *Phys. Fluids A*, Vol. 5, pp. 1092-1094, 1993a.
- [34] Zhou, Y., “*Interacting scales and energy transfer in isotropic turbulence,*” *Phys. Fluids A*, Vol. 5, pp. 2511-2524, 1993b.
- [35] Zhou, Y. 2010, Renormalization group theory for fluid and plasma turbulence, *Phys. Report*, **488**, 1.
- [36] Kraichnan, R.H., “*Inertial range transfer in two- and three-dimensional turbulence,*” *J. Fluid Mech.*, Vol. 47, pp. 525-535, 1971.
- [37] Lesieur, M., *Turbulence in Fluids*, Martinus Nijhoff, Dordrecht, The Netherlands, 1990.
- [38] Gotoh, T., and Watanabe, T., “*Statistics of transfer fluxes of the kinetic energy and scalar variance,*” *J. of Turbulence*, Vol. 6, 33, pp. 1-18, 2005.
- [39] Kaneda, Y., *Renormalization expansions in the theory of turbulence with the use of the Lagrangian position function.* *J. Fluid Mech* 107, 131, 1981.
- [40] Zhou, Y. and Oughton, S., *Nonlocality and the critical Reynolds numbers of the minimum state magnetohydrodynamic turbulence*, *Phys. Plasma*, 18, 072304, 2011.
- [41] Zhou, Y., Buckingham, A.C., Bataille, F., Mathelin, L., *Minimum state for high Reynolds and Peclet number turbulent flows*, *Phys. Lett. A.*, 373, 2746, 2009.
- [42] Domaradzki, J. A., Liu, W., and Brachet, M. E., “*An Analysis of Subgrid-Scale Interactions in Numerically Simulated Isotropic Turbulence,*” *Phys. Fluids A* **5**, 1747, 1993.
- [43] Domaradzki, J. A., Liu, W., Hartel, C., and Kleiser, L., “*Energy Transfer in Numerically Simulated Wall-Bounded Turbulent Flows,*” *Phys. Fluids* **6**, 1583, 1994
- [44] Martinez, D.O., Chen, S., Dolen, G.D., Kraichnan, R.H., Wang, L.P., and Zhou, Y., “*Energy spectrum in the dissipation range of fluid turbulence,*” *J. Plasma Phys.*, 57, 195, 1997.
- [45] Lord Rayleigh, *Scientific Papers* Dover, New York, 1965.
- [46] Taylor, G. I., “*The instability of liquid surfaces when accelerated in a direction perpendicular to their plane,*” *Proc. R. Soc. London, Ser. A* **201**, 192 1950.

- [47] Richtmyer, R. D., “*Taylor instability in shock acceleration of compressible fluids,*” Commun. Pure Appl. Math. **13**, 297 1960.
- [48] Meshkov, E. E. , “*Instability of the interface of two gases accelerated by a shock wave,*” Izv., Acad. Sci., USSR Fluid Dyn. **4**, 101 1969.
- [49] Chandrasekhar, S., *Hydrodynamic and Hydromagnetic Stability*, Dover, New York, 1961.
- [50] Stokes, G.G, On the effect of the internal friction of fluids on the motion of pendulums, Trans. Cambridge Philos. Soc. **9**, 8 1901.
- [51] Lamb, H., *Hydrodynamics* Cambridge University Press, London, 1932.
- [52] Tennekes, H., and Lumley, J.L., *First Course in Turbulence* MIT Press, Cambridge, MA, 1972.
- [53] Hurricane, O.A., Hansen, J.F., Robey, H.F. et al., A high energy density shock driven Kelvin–Helmholtz shear layer experiment, Phys. Plasma, 16, 5, 056305, 2008.
- [54] Haines, B.M., Grinstein, F.F., Welser-Sherrill, L., et al., Analysis of the effects of energy deposition on shock-driven turbulent mixing, Phys. Plasma, 20, 7, 072306, 2013.
- [55] Welser-Sherrill, L., Fincke, J., Doss, F., et al., Two laser-driven mix experiments to study reshock and shear, High Energy Density Phys., 9, 3, 496, [2013](#).
- [56] Haines, B.M., Grinstein, F.F., Welser-Sherrill, L., et al., Simulation ensemble for a laser–driven shear experiment, Phys. Plasma, 20, 9, 092301, 2013.
- [57] Grinstein, F.F., Gowandhan, A.A. et al., On coarse-grained simulations of turbulent material mixing, Physica Scripta, 86, 5, 058203, 2012.
- [58] Smalyk, V.A., Hansen, J.F., Hurricane, O.A., Experimental observations of turbulent mixing due to Kelvin–Helmholtz instability on the OMEGA Laser Facility, Phys. Plasma, 19, 9, 092702, 2012.
- [59] Gowandhan, A.A. and Grinstein, F.F., Numerical simulation of Richtmyer–Meshkov instabilities in shocked gas curtains, J. Turbulence, 12, N43, 2012.

- [60] Hurricane, O.A., Smalyk, V.A., Raman, K., et al., Validation of a Turbulent Kelvin-Helmholtz Shear Layer Model Using a High-Energy-Density OMEGA Laser Experiment, *Phys. Rev. Lett.*, **109**, 15, 2012.
- [61] Di Stefano, C.A., Kuranz, C.C., Keiter, P.A., et al., Late-time breakup of laser-driven hydrodynamics experiments, *High Energy Density Phys.*, **8**, 4, 360, 2012.
- [62] Hurricane, O.A., Smalyk, V.A., Hansen, J.F., et al., Measurements of turbulent mixing due to Kelvin-Helmholtz instability in high-energy-density plasmas, *High Energy Density Phys.*, **9**, 1, 47, 2013.
- [63] Doss, F.W., Loomis, E.N., Welsch-Sherrill, L., et al., Instability, mixing, and transition to turbulence in a laser-driven counterflowing shear experiment, *Phys. Plasma*, **20**, 1, 012707, 2013.
- [64] Drake, R.P., Harding, E.C., and Kuranz, C.C., Approaches to turbulence in high-energy-density experiments, *Physica Scripta*, 2008, 014022, 2008.
- [65] Grinstein, F.F., Margolin, L.G. and Rider, W.G., (Ed.), *Implicit Large Eddy Simulation: Computing Turbulent Flow Dynamics* (New York: Cambridge University Press), 2nd printing 2010.
- [66] Zhou, Y., Grinstein, F.F., Wachtor, A.J., and Haines, B.M., Estimating the effective Reynolds number in implicit large eddy simulation, *Phys. Rev. E*, **89**, 013303, 2014.
- [67] Falkovich, G., Bottleneck phenomenon in developed turbulence, *Phys. Fluids*, **6**, 1411, 1994.
- [68] Yeung, P.K., and Zhou, Y., Universality of the Kolmogorov constant in numerical simulations of turbulence, *Phys. Rev E*, **56**, 1746, 1997.
- [69] She, Z.S., Chen, S., Doolen, G. Kraichnan, R.H. and Orszag, S.A., Reynolds number dependence of isotropic Navier-Stokes turbulence, *Phys. Rev. Lett.*, **70**, 3251, 1993.
- [70] Cao, N., Chen, S., and G. D. Doolen, G.D., Statistics and structures of pressure in isotropic turbulence, *Phys. Fluids* **11**, 2235. 1999

[71] Wang, L.P., Chen, S., Brasseur, J.G., and Wyngaard, J.C., Examination of hypotheses in the Kolmogorov refined turbulence theory through high- resolution simulations, *J. Fluid Mech.* **309**, 113. 1996

[72] Grinstein, F.F. , Gowardhan, A.A., and Wachtor, A.J., “Simulations of Richtmyer-Meshkov Instabilities in Planar Shock-Tube Experiments”, *Physics of Fluids*, **23**, 034106, 2011.

[73] Fureby C. & Grinstein F.F., Monotonically Integrated Large Eddy Simulation of Free Shear Flows, *AIAA Journal*, **37**, 544, 1999.

[74] Porter, D. H., Woodward, P. R., & Pouquet, A., Inertial range structures in decaying turbulent flows. *Phys. of Fluids* **10**, 237, 1998

[75] Fureby C. & Grinstein F.F., Large Eddy Simulation of High Reynolds-Number Free and Wall Bounded Flows, *J. Comput. Phys.*, **181**, 68, 2002